Analysis of Solvability Boundary for Droop-Controlled Microgrids

Chong Wang, *Member, IEEE*, Bai Cui, *Student Member, IEEE* and Zhaoyu Wang, *Member, IEEE*

***Abstract*—The wide-spread integration of renewable energy sources has a great impact on the traditional distribution system. Considering many of these sources are connected to synchronous alternating current (AC) grids via AC inverters with droop controllers, an equivalent model that has a fictitious voltage source with a given voltage phasor is used to represent the AC inverter with droop controllers. With the equivalent model, a sufficient condition based on bus voltage/injected power and system admittance is proposed to analyze the system stress level and distance to solvability boundary of power flow equations. A modified IEEE 123-bus system is used to test the proposed model and the method.**

***Index Terms*—droop-controlled Microgrids, AC inverters, power flow solvability, sufficient condition**

I. Introduction

THE penetration level of renewable energy sources into distribution systems is increasing due to environmental concerns and technological advancements. Many of these sources are small-scale distributed generators (DGs), and microgrids are promising solutions for connecting/controlling these DGs [1]. One common control strategy for microgrids is the droop control, which depends on the principle of power balance [2], relating power changes to the changes of system frequency/voltage magnitude/voltage phase angle [3], [4]. To deal with undesirable voltage/frequency deviations caused by conventional droop controls, washout filter-based power sharing control can be used [5]. The characteristics of droop controls have great impacts on system modeling, operation, and control. One critical impact is on the assessment of the security margins. Usually, the solvability of power flow equations can be used to indicate the system security margins [6]. Since the droop controls change the traditional power flow equations, it is necessary to develop new methods to assess the security margins.

In this letter, we develop a new approach to analyze the security margins for angle droop controlled microgrids. The contributions are twofold: 1) The droop control is equivalent as a fictitious voltage source with a given voltage magnitude and voltage phase angle. 2) With the equivalent model, a sufficient condition based on Levy-Desplanques theorem is used to check power flow solvability of the system. The inputs of this sufficient condition include the system admittance and the present snapshot of bus voltage/injected power. A modified IEEE 123-bus system is used to test the proposed model and the method.

This work was supported by the U.S. Department of Energy Office of Electricity Delivery and Energy Reliability, the National Science Foundation under ECCS 1609080, and Power System Engineering Research Center (PSERC). (*Corresponding author: Zhaoyu Wang*.)

Chong Wang is with the College of Energy and Electrical Engineering, Hohai University, Nanjing 211100, China (e-mail: wangchonghhu@163.com).

Bai Cui is with the School of Electrical and Computer Engineering, Georgia Institute of Technology, Atlanta, GA 30332 USA (email: bcui7@gatech.edu).

Zhaoyu Wang is with the Department of Electrical and Computer Engineering, Iowa State University, Ames, IA 50011, USA (email: wzy@iastate.edu).

II. Network Modeling

This section first shows the network description that shows basic notation for system modeling. Second, the angle droop control laws used in this paper are introduced. Third, the new interpretation for the angle droop control laws is presented to help to analyze the solvability boundary of angle droop-controlled microgrids. Finally, a sufficient condition based on the new interpretation used to check the solvability boundary is provided and how to use it in practice is also presented.

A. Network Description

We consider a system represented by a weighted and connected graph $(\mathcal{B},\mathcal{L})$, in which $\mathcal{B}=\{1,\cdots,n+m+1\}$ is the set of buses and $\mathcal{L}\subseteq\mathcal{B}\times\mathcal{B}$ is the set of lines. Three types of buses are included: inverter buses $\mathcal{I}=\{1,\cdots,n\}$, PQ buses $\mathcal{D}=\{n+1,\cdots,n+m\}$, and a slack bus $\mathcal{S}=\{n+m+1\}$. The line between bus $i\in\mathcal{B}$ and bus $j\in\mathcal{B}$ is weighted by complex admittance $y_{ij}=g_{ij}+\mathrm{j}b_{ij}\in\mathbb{C}^1$, and the whole system is represented by the bus admittance matrix $\mathbf{Y}=\mathbf{G}+\mathrm{j}\mathbf{B}\in\mathbb{C}^{(n+m+1)\times(n+m+1)}$, in which $Y_{ij}=Y_{ji}=-y_{ij}$ and $Y_{ii}=\sum_{j\in\mathcal{B}}y_{ij}$. Each bus i is associated with a voltage magnitude V_i and a voltage phase angle θ_i. For microgrids, the shunt admittance of each bus is ignored. For each bus $i\in\mathcal{B}$, the relations between voltages and active/reactive power injections are represented as follows.

$$P_i=V_i\sum_{j\in\mathcal{B}}V_j(G_{ij}\cos(\theta_i-\theta_j)+B_{ij}\sin(\theta_i-\theta_j)) \tag{1a}$$

$$Q_i=V_i\sum_{j\in\mathcal{B}}V_j(G_{ij}\sin(\theta_i-\theta_j)-B_{ij}\cos(\theta_i-\theta_j)) \tag{1b}$$

where P_i and Q_i are injected active power and reactive power, respectively. G_{ij} and B_{ij} are the (i,j)th elements of the matrices $\mathbf{G}$ and $\mathbf{B}$, respectively.

B. Grid-Side Model of Droop Control

The grid-side model of droop control at bus i can be represented as a controllable voltage source, and the droop control can be expressed as follows.

$$\sigma_{\theta_i}(P_i^*-P_i)+\theta_i^*-\theta_i=0 \tag{2a}$$

$$\sigma_{V_i}(Q_i^*-Q_i)+V_i^*-V_i=0 \tag{2b}$$

where (2a) and (2b) are the angle droop and voltage droop control laws [4] that are investigated in this letter. P_i^* and Q_i^* are rated active/reactive power for the droop control at the bus i, and V_i^* and θ_i^* are the rated voltage magnitude and phase angle when the inverter supplies the grid to its rated active/reactive power P^* and Q^*, and σ_{V_i} and σ_{θ_i} are the voltage and angle droop gains. The angle (voltage) droop gain relates the angle (voltage) difference between the inverter and the connection point to the difference between actual injected active (reactive) power and rated injected active (reactive) power.

C. New Interpretation of Droop Control Laws

The droop control laws in (2a) and (2b) are derived from the full power flow equations (1a) and (1b) based on the assumptions that $V_i \approx 1$ and $\theta_i \approx 0$ for all buses. With the assumptions, we have the following full power flow counterparts.

$$\theta_i^* - \theta_i \approx V_i V_i^* \sin(\theta_i^* - \theta_i) \tag{3a}$$

$$\begin{aligned} V_i^* - V_i &\approx V_i^* \cos(\theta_i^* - \theta_i) - V_i \\ &\approx V_i(V_i^* \cos(\theta_i^* - \theta_i) - V_i) \end{aligned} \tag{3b}$$

With (3a)-(3a), the equations (2a) and (2b) can be approximated as follows.

$$\sigma_{\theta_i}(P_i^* - P_i) + V_i V_i^* \sin(\theta_i^* - \theta_i) = 0 \tag{4a}$$

$$\sigma_{V_i}(Q_i^* - Q_i) + V_i(V_i^* \cos(\theta_i^* - \theta_i) - V_i) = 0 \tag{4b}$$

where (4a) and (4b) are equations regarding active power flow and reactive power flow, respectively. The parameters σ_{θ_i} and σ_{V_i} can be considered as line reactances with respect to the active and reactive power equation, respectively. However, σ_{θ_i} and σ_{V_i} should be equal under this model. To make (4a) and (4b) have practical physical meanings, we introduce an equivalent reactance $\sigma_i = \max\{\sigma_{\theta_i}, \sigma_{V_i}\}$ to replace σ_{θ_i} and σ_{V_i} in (4a) and (4b). We pick the maximum of the two as the line reactance since increasing line impedance generally decreases system stability margin [7]. This means that $\sigma_i = \min\{\sigma_{\theta_i}, \sigma_{V_i}\}$ results in an overestimated loading margin and $\sigma_i = \max\{\sigma_{\theta_i}, \sigma_{V_i}\}$ causes an underestimated loading margin. To ensure the feasible loading margin, we should choose $\sigma_i = \max\{\sigma_{\theta_i}, \sigma_{V_i}\}$ producing an underestimated loading margin.

With the introduced reactance σ_i, we have the following approximate algebraic equations:

$$\sigma_i(P_i^* - P_i) + V_i V_i^* \sin(\theta_i^* - \theta_i) = 0 \quad i \in \mathcal{I} \tag{5a}$$

$$\sigma_i(Q_i^* - Q_i) + V_i(V_i^* \cos(\theta_i^* - \theta_i) - V_i) = 0 \quad i \in \mathcal{I} \tag{5b}$$

$$P_i - P_{i,D} = 0 \quad i \in \mathcal{D} \tag{5c}$$

$$Q_i - Q_{i,D} = 0 \quad i \in \mathcal{D} \tag{5d}$$

where $P_{i,D}$ and $Q_{i,D}$ are active power and reactive power of load at the bus i, respectively. The model with the full power flow counterparts in (5) can be interpreted as connecting a fictitious voltage source with voltage magnitude V_i^* and voltage angle θ_i^* to the inverter bus $i \in \mathcal{I}$ via a line with reactance j(σ_i). Therefore, the model (5) is equivalent to an augmented system in which there are $n + m$ constant power buses (n inverter buses and m load buses) and $n + 1$ voltage-controlled buses (n fictitious buses and 1 slack bus). Fig. 1 (a) and (b) show an original droop-controlled microgrid and its equivalent system with the fictitious voltage source.

D. Condition for Power Flow Solvability

For the equivalent system from the original droop-controlled microgrid, we define $\mathcal{F}$ as the set of fictitious buses, and the system equations can be expressed as follows.

$$\begin{bmatrix} I_{\mathcal{S}'} \\ I_{\mathcal{D}'} \end{bmatrix} = \begin{bmatrix} Y_{\mathcal{S}'\mathcal{S}'} & Y_{\mathcal{S}'\mathcal{D}'} \\ Y_{\mathcal{D}'\mathcal{S}'} & Y_{\mathcal{D}'\mathcal{D}'} \end{bmatrix} \begin{bmatrix} V_{\mathcal{S}'} \\ V_{\mathcal{D}'} \end{bmatrix} \tag{6}$$

where $\mathcal{S}' = \{\mathcal{S}, \mathcal{F}\}$ and $\mathcal{D}' = \{\mathcal{D}, \mathcal{I}\}$. $I_{\mathcal{S}'}$ and $I_{\mathcal{D}'}$ are the injected current vectors. $V_{\mathcal{S}'}$ and $V_{\mathcal{D}'}$ are bus voltage vectors. Based on (6), we have the equation

$$V_{\mathcal{D}'} = E_{\mathcal{D}'} - Z_{\mathcal{D}'\mathcal{D}'} I_{\mathcal{D}'} \tag{7}$$

where $E_{\mathcal{D}'} = -Y_{\mathcal{D}'\mathcal{D}'}^{-1} Y_{\mathcal{D}'\mathcal{S}'} V_{\mathcal{S}'}$ and $Z_{\mathcal{D}'\mathcal{D}'} = -Y_{\mathcal{D}'\mathcal{D}'}^{-1}$.

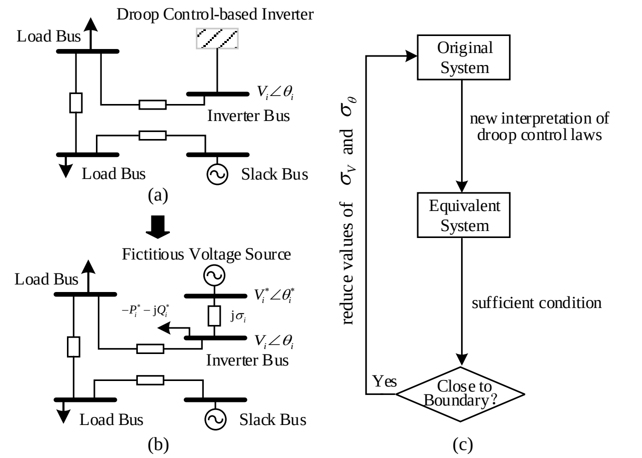

Fig. 1. (a) Original system. (b) Equivalent system. (c) Flowchart of the proposed model.

The Jacobian matrix of the model (1a)-(1b) where we have $i \in \mathcal{D}'$ can be expressed as follows.

$$J = \begin{bmatrix} \partial P/\partial \theta & \partial P/\partial V \\ \partial Q/\partial \theta & \partial Q/\partial V \end{bmatrix} \tag{8}$$

The sufficient condition for power flow solvability is that the Jacobian J is nonsingular. Based on the chain rule, the singularity of J coincides with that of the following Jacobian matrix [8], [9].

$$J' = \begin{bmatrix} \partial P/\partial I_R & \partial P/\partial I_I \\ \partial Q/\partial I_R & \partial Q/\partial I_I \end{bmatrix} \tag{9}$$

where I_R and I_I are real and imaginary parts of current.

Based on our previous work [8], the sufficient condition for the nonsingular J is

$$|V_{\mathcal{D}'}(k)| > \sum_{k' \in \mathcal{D}'} \frac{|Z_{\mathcal{D}'\mathcal{D}'}(k, k')| \cdot |S_{\mathcal{D}'}(k')|}{|V_{\mathcal{D}'}(k')|} \tag{10}$$

where $S_{\mathcal{D}'}$ is the power injection vector of buses belonging to the set $\mathcal{D}'$. The terms (k) and (k') denote the kth and the k'th elements of the corresponding vectors, the term (k, k') means the (k, k')th element of the corresponding matrix. To obtain this condition, we first use Wirtinger Calculus [10] to transform the power flow Jacobian (9) to a complex matrix, and then apply Levy-Desplanques theorem [8].

We define an index R as follows.

$$R_{\mathcal{D}'} = |V_{\mathcal{D}'}(k)| \Bigg/ \sum_{k' \in \mathcal{D}'} \frac{|Z_{\mathcal{D}'\mathcal{D}'}(k, k')| \cdot |S_{\mathcal{D}'}(k')|}{|V_{\mathcal{D}'}(k')|} \tag{11}$$

According to the sufficient condition, the system is within the solvability boundary when $R_{\mathcal{D}'} > 1$. The proximity of the indicator to 1 can be viewed as an indication of the distance to solvability boundary.

In practice, an angle droop-controlled microgrid can be transformed into an equivalent system by means of the new interpretation of droop control laws in Section II.C firstly. Then, the sufficient condition in Section II.D is used to analyze if the system is close to the solvability boundary. If yes, we can reduce the parameter σ_{V_i} and σ_{θ_i} in the droop control to increase the distance of the operating point to the solvability boundary. The flowchart of this process is shown in Fig. 1 (c).

III. Case Studies

The effectiveness of the model is tested on a modified IEEE 123-bus system [11] with different droop-controlled inverters. In simulations, V^*, θ^*, P^*, and Q^* are set to be 0.95, -0.1, 0.01 and 0.01 (p.u.), respectively. Table I shows the comparison results with different droop-controlled inverters under different algorithms. The second column gives the locations of inverters. The third column shows the critical loading factors of the original system. These critical loading factors are obtained based on power flow calculation (PFC) of the original system. The critical loading factor is defined as the largest loading factor where power flow equations can be solved. The fourth column and the fifth column present the critical loading factors of the equivalent system based on PFC and the sufficient condition (SC) used in this paper, respectively. It is observed that the critical loading factor for the equivalent system based on the sufficient condition can be used to approximately check the power flow solvability of the original system. Fig. 2 shows the values of $\log_{10}(R)$ with respect to different loading factors when having five droop-controlled inverters. It is observed that the index decreases with increasing loading factors.

TABLE I
Critical Loading Factor with Different Scenarios

No.	Buses with Droop-controlled Inverters	Original System (PFC)	Equivalent System (PFC)	Equivalent System (SC)
S1	9	4.244	4.227	4.166
S2	9, 15	4.294	4.291	4.226
S3	9, 15, 18	4.394	4.385	4.319
S4	9, 15, 18, 24	4.462	4.461	4.393
S5	9, 15, 18, 24, 32	4.536	4.514	4.458
S6	9, 15, 18, 24, 32, 35	4.495	4.492	4.433
S7	9, 15, 18, 24, 32, 35, 38	4.525	4.523	4.462

Fig. 3 shows the critical loading factors with different assumptions on equivalent σ. The red curve and the blue curve represent $\sigma = \min\{\sigma_V, \sigma_\theta\}$ and $\sigma = \max\{\sigma_V, \sigma_\theta\}$, respectively. For these two assumptions, one is relaxed and the other is conservative. It is observed that the critical loading factors based on the assumption $\sigma = \min\{\sigma_V, \sigma_\theta\}$ are larger than those based on the assumption $\sigma = \max\{\sigma_V, \sigma_\theta\}$. This indicates that the assumption $\sigma = \min\{\sigma_V, \sigma_\theta\}$ makes the corresponding critical loading factors relaxed. To ensure power flow solvability of the original model, we should select the conservative assumption. This justifies our choice of $\sigma = \max\{\sigma_V, \sigma_\theta\}$.

Fig. 4 shows the critical loading factors with different σ_V and σ_θ. It is observed that the critical loading factors increase when the values of σ_V and σ_θ decrease. This indicates that the distance of the operating point to solvability boundary increase when the values of σ_V and σ_θ decrease. In practical systems, we can analyze the distance to solvability boundary based on the proposed model and the sufficient condition. If the operating point is close to solvability boundary, we can reduce the values of σ_V and σ_θ to increase the distance to solvability boundary.

IV. Conclusions

This letter proposes a new approach to analyze solvability boundary of the droop-controlled microgrids. An equivalent model, i.e., a fictitious voltage source, is used to represent the droop controls of AC inverters in microgrids. With the equivalent model, a sufficient condition that uses the system admittance and the present voltage/injected power is used to indicate distance to solvability boundary. A modified IEEE 123-bus system is used to validate the proposed model.

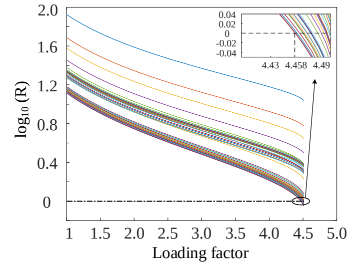

Fig. 2. The values of $\log_{10}(R)$ with different loading factors.

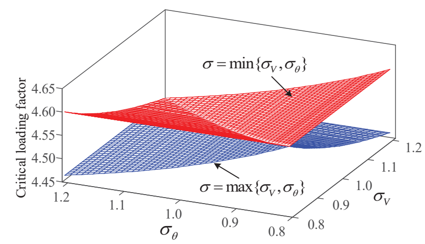

Fig. 3. Critical loading factors with different assumptions on σ.

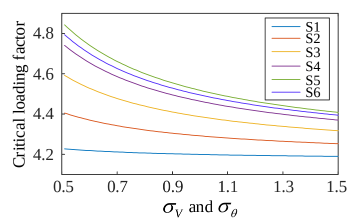

Fig. 4. Critical loading factors with different values of σ.

References

[1] M. Yazdanian and A. Mehrizi-Sani, "Distributed control techniques in microgrids," *IEEE Trans. Smart Grid*, vol. 5, no. 6, pp. 2901–2909, Nov. 2014.

[2] P. Kundur, *Power system stability and control*, McGraw-Hill, 1944.

[3] E. Barklund, N. Pogaku, M. Prodanovic, C. Hernandez-Aramburo, and T. C. Green, "Energy management in autonomous microgrid using stability-constrained droop control of inverters," *IEEE Trans. on Power Electronics*, vol. 23, no. 5, pp. 2346–2352, Sep. 2008.

[4] R. Majumder, B. Chaudhuri, A. Ghosh, R. Majumder, G. Ledwich, and F. Zare, "Improvement of stability and load sharing in an autonomous microgrid using supplementary droop control loop," *IEEE Trans. Power Syst.*, vol. 25, no. 2, pp. 796–808, May 2010.

[5] M. Yazdanian and A. Mehrizi-Sani, "Washout filter-based power sharing," *IEEE Trans. Smart Grid*, vol. 7, no. 2, pp. 967–968, Mar. 2016.

[6] T. J. Overbye, "A power flow measure for unsolvable cases," *IEEE Trans. Power Syst.*, vol. 9, no. 3, pp. 1359–1365, Aug. 1994.

[7] J. W. Simpson-Porco, F. Drfler, and F. Bullo, "Voltage collapse in complex power grids," *Nature Communications*, vol. 7, Feb. 2016.

[8] Z. Wang, B. Cui, and J. Wang, "A necessary condition for power flow insolvability in power distribution systems with distributed generators," *IEEE Trans. Power Syst.*, vol. 32, no. 2, pp. 1440–1450, Mar. 2017.

[9] C. Wang, A. Bernstein, J. Y. L. Boudec, and M. Paolone, "Explicit conditions on existence and uniqueness of load-flow solutions in distribution networks," *IEEE Trans. Smart Grid*, vol. 9, no. 2, pp. 953–962, Mar. 2018.

[10] R. Remmert, *Theory of Complex Functions*, New York, NY, USA: Springer-Verlag, 1991.

[11] S. Bolognani, "Approx-pfapproximate linear solution of power flow equations in power distribution networks," 2015. [Online]. Available: https://github.com/saveriob/approx-pf